Journal of ELECTRONIC MATERIALS, Vol. 39, No. 9, 2010
DOI: 10.1007/s11664-009-0977-y

Self-Assembled Germanium Quantum-Dot Supercrystals in Silicon with Extremely Low Thermal Conductivities for Thermoelectrics

JEAN-NUMA GILLET[1,3] and SEBASTIAN VOLZ[2]

1.—Institut d'Electronique, de Microélectronique et de Nanotechnologie (IEMN, CNRS UMR 8520), Dept. of Physics, Université de Lille 1, Av. Poincaré, BP 60069, 59652 Villeneuve d'Ascq Cedex, France. 2.—Laboratoire d'Energétique Moléculaire et Macroscopique, Combustion (EM2C, CNRS UPR 288), Ecole Centrale Paris, Grande Voie des Vignes, 92295 Châtenay-Malabry Cedex, France. 3.—e-mail: jngillet@gmail.com

Superlattices with one-dimensional (1D) phonon confinement were studied to obtain a low thermal conductivity for thermoelectrics. Since they are composed of materials with a lattice mismatch, they often show dislocations. Like 1D nanowires, they also decrease heat transport in only one main propagation direction. It is therefore challenging to design superlattices with a thermoelectric figure of merit ZT higher than unity. Epitaxial self-assembly is a major technology to fabricate three-dimensional (3D) Ge quantum-dot (QD) arrays in Si. They have been used for quantum and solar-energy devices. Using the atomic-scale phononic crystal model, 3D Ge QD supercrystals in Si also present an extreme reduction of the thermal conductivity to a value that can be under 0.04 W/m/K. Owing to incoherent phonon scattering, the same conclusion holds for 3D supercrystals with moderate QD disordering. As a result, they might be considered for the design of highly efficient complementary metal–oxide–semiconductor (CMOS)-compatible thermoelectric devices with ZT possibly much higher than unity. Such a small thermal conductivity was only obtained for two-dimensional layered WSe_2 crystals in an experimental study. However, electronic conduction in the Si/Ge compounds is significantly enhanced. The 0.04 W/m/K value can be computed for different Ge QD filling ratios of the Si/Ge supercrystal with size parameters in the range of current fabrication technologies.

Key words: Thermoelectrics, thermal conductivity, self-assembly, quantum dot, silicon, germanium

INTRODUCTION

The energy-conversion efficiency of a thermoelectric material is an increasing function of its thermoelectric figure of merit ZT, which is inversely proportional to its thermal conductivity λ and directly proportional to its power factor ($S^2\sigma$). Indeed, when S, σ, and T denote the Seebeck coefficient, electrical conductivity, and absolute temperature, respectively, the nondimensional ZT is given by $ZT = S^2\sigma T/\lambda$.[1,2] Discovery of a material with ZT higher than 3 would produce a thermoelectric yield that is higher than 42% of the Carnot efficiency for hot and cold junctions at 800 K and 300 K, respectively. Such a breakthrough could have an enormous impact for energy conversion and renewable energies. To achieve this dream, the design of semiconducting materials with an indirect electronic bandgap showing a very low thermal conductivity is currently one of the major areas of research in solid-state physics and chemistry.[1–11]

Superlattices made up of periodic thin semiconducting layers were the first type of nanomaterials to be studied with the purpose of achieving $ZT > 1$.

(Received June 26, 2009; accepted October 20, 2009; published online November 10, 2009)

The superlattice thermal conductivity can be significantly reduced compared with bulk material due to the possible one-dimensional (1D) phonon confinement between its layer interfaces.[9,10] However, the design of a material with ZT larger than unity is usually not possible with many superlattices. Indeed, the lattice mismatch at their layer interfaces forms dislocations that often lead to cracks owing to high residual stresses from covalent bonds stopping dislocation propagation. These defects lead to σ reduction and prevent ZT increase above unity. Recently, nanowires were also proposed for thermal conductivity reduction.[3–5] Nevertheless, like the superlattices, they decrease thermal transport in only one propagation direction. Therefore phonon confinement, as for nonfocusing and localization, cannot be as significant as in three-dimensional (3D) nanostructured materials. Experimentally, these 1D materials for thermal insulation usually fail to beat the lowest amorphous limit of bulk Si of around 1 W/m/K.[11]

With the spectacular development of nanotechnology, self-assembly became a major technology for bottom-up synthesis of 3D nanostructured devices for various applications in drug design, biotechnologies, electronics, and photonics, for instance.[12–15] Self-assembly of epitaxial layers on silicon has been used to fabricate 3D Ge quantum-dot (QD) arrays in diamond-cubic (dc) Si for quantum-device and solar-energy applications.[16,17] In this theoretical study, we show based on the atomic-scale 3D phononic crystal model[18] that high-density 3D arrays of self-assembled (SA) Ge QDs surrounded by a dc Si matrix can also present an extreme reduction of the thermal transport. Gillet showed in 3D Ge-QD supercrystals in Si with different germanium concentrations that the thermal conductivity can be lower than 0.04 W/m/K at room temperature, or less than twice that of air.[19] This quantity represents a 3750-fold reduction factor with respect to bulk dc Si (150 W/m/K). As a result, these 3D Si/Ge QD supercrystals, with two scales of texture, could be considered for the design of very efficient thermoelectric devices showing compatibility with CMOS microelectronics. A thermal conductivity with a similar value of 0.05 W/m/K was obtained in a preceding experimental study of two-dimensional (2D) disordered layered WSe_2 crystals.[6] This value also shows a significant reduction with respect to the extreme low limit of amorphous WSe_2 of the order of 0.3 W/m/K.[6,20] Nevertheless, owing to the better electrical properties of silicon-based devices and high germanium electronic mobility, electronic transport in the Si/Ge crystals can be significantly enhanced compared with that in WSe_2 crystals. The importance of electrical doping, which might be another increase factor of ZT in the Si/Ge crystals, is still an open question. Indeed, from the Wiedemann–Franz law, doping increases both electrical conductivity σ and electronic thermal conductivity λ_e, which might become nonnegligible with respect to the lattice thermal conductivity (studied in this paper) for high carrier concentrations, resulting in a possibly negative effect on the increase of ZT. However, a recent theoretical study of the electronic properties of silicon nanowires with *ab initio* and density functional theory (DFT) calculations showed that ZT could be significantly enhanced by electrical doping in a carrier concentration range from 10^{16} cm^{-3} to 10^{20} cm^{-3}.[21] In fact, the maximum of ZT in this range depends on geometrical properties such as the growth crystallographic axis and nanowire diameter.

The phonon harmonic behavior in the atomic-scale 3D phononic crystal is modeled from its dispersion curves, which are computed in a range from 0 THz to 20 THz by lattice dynamics.[22–24] Three acoustical branches start from 0-Hz eigenfrequencies in our discrete model. The folded optical branches are populated at low temperatures. Indeed, at a frequency $\nu \sim 1$ THz, the ratio $k_B T/(h\nu)$ is higher than 10% for $T \geq 5$ K (with the Boltzmann and Planck constants k_B and h, respectively). Flat dispersion curves with mini bandgaps are obtained for the higher-energy folded modes. This phenomenon leads to much smaller phonon group velocities than those of bulk dc Si. The huge decrease of the thermal conductivity in the atomic-scale 3D phononic crystal is not only due to the effect of the low phonon group velocities. Additional incoherent effects of phonon multiple scattering between the Ge QDs have to be considered in a diffusive model owing to a wave-particle duality appearing when the folded phonon wavelengths are smaller than the double lattice constant $2d$ of the supercells in the Si/Ge QD supercrystal. Multiple scattering of the diffused phonons breaks their mean free paths (MFPs) and constitutes another thermal-conductivity reduction factor in the QD supercrystal. Incoherent scattering can be modeled using a near-field theory such as that of van de Hulst and other authors.[25–27] Owing to its predominance, strong nonfocusing and localization effects of the phonons appear. Indeed, the density of thermal paths is low, owing to the two scales of texture in the 3D Si/Ge QD supercrystal. Thus, the supercrystal thermal conductivity can be much lower than that of the lowest amorphous limits of related bulk materials such as Si or WSe_2. In fact, the heat flux can find a larger number of random thermal paths in amorphous materials, as obtained experimentally in Ref. 6. Based on the above, the same extreme reduction of the thermal conductivity holds for 3D Si/Ge QD supercrystals if the degree of QD disordering remains moderate with respect to an amorphous Si/Ge material.

In first numerical results, we show for a wide temperature range that the thermal conductivity decreases for increasing QD filling ratio x (in Ge at.%) in the case of a supercell with constant average distance d between the Ge QDs. In an atomic-scale 3D phononic crystal where each supercell is made up of a QD with 1332 Ge atoms inside a cage

of 1412 Si atoms, the thermal conductivity can be decreased by a factor of 750 or more compared with bulk dc Si, or below the upper limit of only 0.2 W/m/K. This value is five times smaller than the Einstein limit of around 1 W/m/K for disordered bulk Si.[20] Thereafter, we present the size dependence of the thermal conductivity λ versus the average distance d between the QDs. A λ decrease with a power-law dependence is observed with increasing d. This analysis enables Gillet to predict that λ can be lower than 0.04 W/m/K for two different QD filling ratios x at room temperature.[19] For instance, when x = 12.5 Ge at.% or x = 48.5 Ge at.%, the d-values to obtain the same λ = 0.04 W/m/K are 19.6 nm or 7.6 nm, respectively. The presented numerical results might have a significant impact for thermoelectrics and forthcoming fabrication of a 3D Ge/Si supercrystal.

ATOMIC-SCALE 3D PHONONIC CRYSTAL MODEL

Confinement from Flat Dispersion Curves

To investigate the extreme thermal conductivity reduction of 3D high-density arrays of SA Ge QDs in a dc Si matrix, we propose the atomic-scale 3D phononic crystal model with a supercrystal lattice constant $d = Na$ given by an integer number of interatomic distances a in the $\langle 100 \rangle$ directions. As shown in Fig. 1, a period of this phononic-like crystal is made up of a group of $N \times N \times N = N^3$ dc Si cells. Therefore, the N^3 dc primitive cells form a larger cubic supercell in a simple-cubic (sc) supercrystal. When N = 7, as depicted in Fig. 1, each supercell is composed of N^3 = 343 dc primitive cells. In this example, the possible phononic-like crystals have a nonrelaxed $d = Na = 7a$ = 3.8017 nm, where a = 0.5431 nm is the lattice constant of bulk dc Si. The total number of atoms forming a supercell is $8N^3$ = 2744, since the number of atoms per primitive cubic cell is 8 in the dc subgroup. At each supercell center, we substitute a number of Si atoms by Ge atoms to obtain a 3D Ge/Si nanocomposite. In five possible atomic configurations with N = 7, we substitute the Si atoms contained in a subset of $M \times M \times M = M^3$ dc primitive cells, located at each supercell center, by Ge atoms to form Ge QDs (with a box-like nanoparticle shape) with different bases $w = Ma$. The number of dc Ge inter-atomic distances is M = 1, 2, 3, 4 or 5 in the $\langle 100 \rangle$ symmetric directions.

When the size parameter M is equal to 1, 2, 3, 4 or 5, the central dc Ge QD in each supercell contains 28, 126, 344, 730 or 1332 Ge atoms, respectively. They are surrounded by 2716, 2618, 2400, 2014 or 1412 Si atoms, respectively. The example with M = 5 refers to the largest QD basis $w = Ma = 5a$ = 2.7155 nm among the defined 3D Si/Ge QD supercrystals with supercrystal lattice constant $d = Na = 7a$ = 3.8017 nm. In this case (N = 7, M = 5), each supercell is composed, at its center, of a dc Ge QD composed of M^3 = 125 primitive dc Ge cells. They are surrounded by $N^3 - M^3$ = 218 peripheral dc Si cells, as in the discrete-medium scheme of Fig. 1b. In this figure, the Ge and Si atom locations in the supercell are shown in black and light (yellow) colors, respectively. The periodic spatial repetition of supercells creates an atomic-scale 3D phononic crystal, as in the continuous-medium scheme of Fig. 1a. The overall chemical compositions Ge_xSi_{1-x} of the five QD supercrystal configurations with the reduced supercell lattice constant N = 7 are obtained from the Ge-QD filling ratios x = 1.02 Ge at.%, 4.59 Ge at.%, 12.53 Ge at.%, 26.60 Ge at.%,

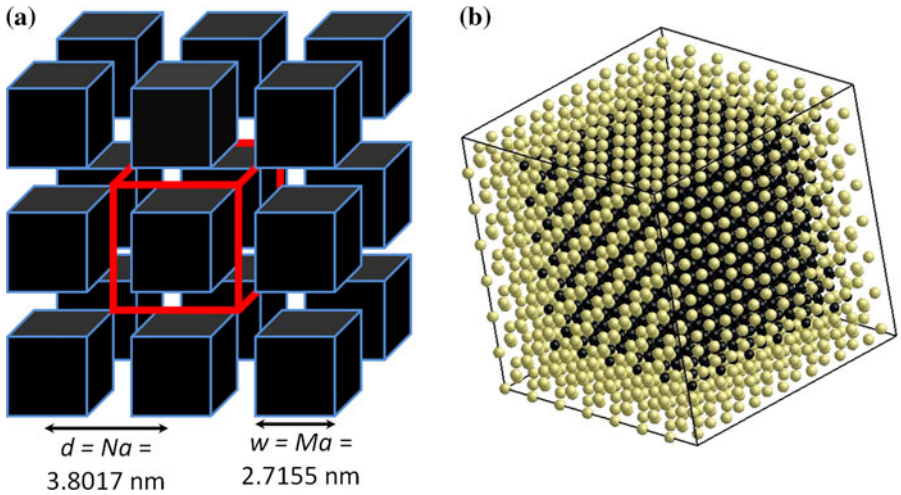

Fig. 1. (Color online) Schematics at two different scales of an atomic-scale 3D phononic crystal with N = 7 and M = 5. In the continuous medium-like drawing in (a), the quantum dots (QDs) with an edge length of $w = 5a$ = 2.7155 nm and spacing of $d = 7a$ = 3.8017 nm are displayed as ordered black cubes with highlighted (blue) edges. In (a), the transparent central cube with thick highlighted (red) edges shows one of the nanomaterial supercells. The discrete medium-like drawing of a supercell is presented in (b). The 1332 Ge atoms forming a QD with a box-like nanoparticle shape in (a) are shown in black in (b), while the 1412 peripheral Si atoms are shown in light (yellow) color in the remainder of the supercell.

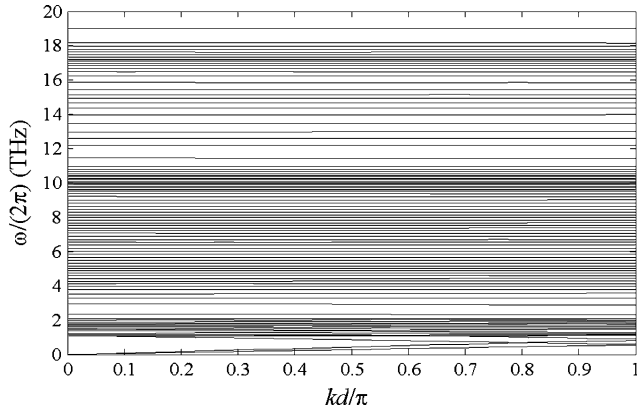

Fig. 2. One hundred and two branches chosen among the 8232 dispersion curves of an atomic-scale 3D phononic crystal with $M = 5$ and $N = 7$ ($d = 3.8017$ nm); equivalent crystallographic directions ⟨100⟩.

and 48.54 Ge at.% for the reduced QD bases $M = 1$, 2, 3, 4, and 5, respectively. As shown in Fig. 1a and b, the 3D QD supercrystal shows two scales of texture: The first is defined by the interatomic distance a between the primitive atoms forming a supercell while the second, larger scale is given by the distance $d = Na$ between the Ge QDs.

Since $N_m = 3 \times 8 \times N^3 = 8232$ is the number of vibration degrees of freedom in a supercell with the reduced supercrystal lattice constant $N = 7$, lattice dynamics is used to compute the 8232 dispersion curves of the five Si/Ge QD supercrystals with $N = 7$ from their N_m phonon eigenmodes.[22] The empirical Stillinger–Weber potential is preferred to describe the binding energy between two and three neighbor atoms.[23,24] The equilibrium relaxed positions of the atoms in each supercell as a function of the masses and elastic constants of dc Si and Ge are obtained by numerical minimization before lattice dynamics. Since the dispersive effect of each atom in a supercell is considered in this discrete model, the supercrystal dispersion curves are obtained in a frequency range from 0 THz to ~20 THz. Figure 2 shows 102 of the 8232 computed dispersions curves of an atomic-scale 3D phononic crystal with the size parameters $N = 7$ and $M = 5$ (sketched in Fig. 1). The $N^3 - 3 = 8229$ folded optical curves are usually very flat. This harmonic phenomenon results in very low group velocities since they are obtained by derivation of the dispersion branches with respect to the wavenumber in a particular direction. The low group velocities constitute a first effect on the extreme thermal-conductivity decrease observed in the Si/Ge QD supercrystals, as explained in the following.

Thermal Conductivity Model

Using the general integration (Eq. 1) over the radial wavenumber $k = |\mathbf{k}|$, as demonstrated in Ref. 18 without using the Debye approximation, we derive the thermal conductivity λ of a 3D crystalline material with a cubic symmetry from its phonon scattering relaxation times $\tau_{k,m}$ and dispersion curves, computed with lattice dynamics (see the "Confinement from Flat Dispersion Curves" section):

$$\lambda = \frac{1}{3}\sum_{m=1}^{N_m}\int_0^{k_{\max}} \tau_{k,m}(v_{k,m})^2 \hbar\omega_{k,m}\frac{\partial n_{k,m}^{(0)}(T)}{\partial T} g_k \, \mathrm{d}k. \quad (1)$$

In Eq. 1, $\hbar = h/(2\pi)$ is the reduced Planck constant, and m is the index of one branch of the N_m dispersion curves to which the mode (k, m) belongs. We recall that the number of eigenvalues is given by $N_m = 24N^3 = 8232$ for an atomic-scale 3D phononic crystal with the reduced supercrystal lattice constant $N = 7$. The Bose–Einstein distribution of the phonons is denoted by $n_{k,m}^{(0)}(T)$ in Eq. 1 for an equilibrium system temperature T. The radial group velocities $v_{k,m} = \partial\omega_{k,m}/\partial k$ (Eq. 1) are obtained by derivation of the dispersion curves with respect to k. We also point out that the phonon MFPs $l_{k,m}$ can be derived from $l_{k,m} = \tau_{k,m}v_{k,m}$. In Eq. 1, g_k is the free-particle density of states (DOS) per volume unit as a function of k. The integral (Eq. 1) is taken over the finite interval $[0, k_{\max}]$, where $k_{\max}$ is the right border of the first folded Brillouin zone (BZ). For a bulk face-centered cubic (fcc) material, this boundary is given by $k_{\max} = 2\pi/a$, with the lattice constant $a = 0.5431$ nm for bulk dc Si. Differently, owing to the sc crystallinity at the largest scale of the Ge QDs, $k_{\max} = \pi/d$ is used in Eq. 1 to obtain the thermal conductivity λ of a Si/Ge QD supercrystal with average distance $d = Na$ between the QDs. In the example of Fig. 1, for a reduced supercrystal lattice constant $N = 7$, the width of the folded BZ is only $1/(2N) = 1/14$ of that of bulk dc Si since $(2\pi/a)/(\pi/d) = 2d/a = 2N = 14$.

Shrunk Relaxation Times from Incoherent Scattering

To compute the thermal conductivity λ of the atomic-scale 3D phononic crystal (Eq. 1), an analytical model of the total phonon relaxation times $\tau_{k,m} = l_{k,m}/v_{k,m}$ of the modes (k, m) is implemented from the Matthiessen rule and scattering cross-sections in a "phonon-particle" approach. Only incoherent scattering processes have to be considered. Indeed, the $N^3 - 3$ folded dispersion curves, for which the scattering cross-sections are the largest, have folded phonon wavelengths smaller than the double supercell period $2d$. As a result, the (non-normalized) overall scattering probability $1/\tau_{k,m}$ can be defined from the Mathieussen rule as a summation of two incoherent scattering probabilities:

$$\frac{1}{\tau_{k,m}} = \frac{1}{\tau_{k,m}^{(\mathrm{u})}} + \frac{1}{\tau_{k,m}^{(\mathrm{p})}}. \quad (2)$$

In Eq. 2, the contribution $1/\tau_{k,m}^{(\mathrm{d})}$ of isotopes and atomic-size defects can be neglected. Indeed, this term is a second-order effect in high-purity dc Si.

To compute the scattering probability $1/\tau_{k,m}^{(u)}$ of the umklapp (or U) process, a common formulation given in Refs. 28 and 29, depending on T, is utilized. Based on the above, the free-particle DOS per volume unit (Eq. 1) is defined as $g_k = k^2/\pi^2$ instead of $k^2/(2\pi^2)$ in bulk dc Si with six dispersion curves, as discussed in Ref. 18. In Eq. 2, the multiple-scattering probability $1/\tau_{k,m}^{(p)}$ between the Ge QDs is an incoherent effect resulting from nonfocusing and localization of the phonons with small wavelengths and group velocities.

Solving this multiple-scattering problem is highly computationally demanding in three dimensions. An approximated method to obtain $1/\tau_{k,m}^{(p)}$ (Eq. 2) from the scattering cross-section $\sigma_{k,m}^{(p)}$ versus (k, m) has to be used. The quantum perturbation approach of Kim and Majumdar[25] is chosen in this study to obtain an approximated analytical model $\sigma_{k,m}^{(p')}$ of the cross-sections $\sigma_{k,m}^{(p)}$ of the scatters (i.e., the Ge QDs). This method considers each scatter individually in the framework of a decoupling approximation when their cross-sections remain smaller than the van de Hulst's geometrical limit $2\pi\bar{R}^2$ with the scatter average radius $\bar{R}$. Therefore, owing to BZ folding, the scatter cross-sections $\sigma_{k,m}^{(p')}$ of the $N^3 - 3$ folded optical modes are assigned in this paper to the same analytical formulations $\sigma_{k,m}^{(p')} \equiv \sigma_{k,m}^{(ac)}$, with $m = 1$ to 3, as those of the three nonfolded acoustical modes. This acoustic-like approach leads to an underestimate $\sigma_{k,m}^{(ac)} < \sigma_{k,m}^{(p')}$ of the scatter cross-sections. Indeed, the quantity $\sigma_{k,m}^{(ac)}$ is computed in the first half BZ and related to scattering of the three nonfolded acoustical modes. Nevertheless, this approximation enables us to compute an upper limit $\lambda_{max} > \lambda_{real}$ for the thermal conductivity λ of the 3D Si/Ge QD supercrystal. Indeed, the relaxation times $\tau_{k,m}^{(p)}$ (Eq. 2) are set to their overestimated values given by $\tau_{k,m}^{(ac)}$. As a result, the quantity λ in Eq. 1 is maximized from the inequality $\tau_{k,m}^{(ac)} > \tau_{k,m}^{(p')}$ that holds for any mode (k, m) since

$$1/\tau_{k,m}^{(ac)} = \eta\sigma_{k,m}^{(ac)}v_{k,m} \text{ and } 1/\tau_{k,m}^{(p')} = \eta\sigma_{k,m}^{(p')}v_{k,m} \text{ leading to } \tau_{k,m}^{(ac)} > \tau_{k,m}^{(p')}, \quad (3)$$

where $\eta = 1/d^3$ is the QD volumic density in (m^{-3}) in the supercrystal.[25]

The quantity $\sigma_k^{(p')}$, when taken as a function of only k, connects the Rayleigh-type far-field $\left(\sigma_k^{(F\ Field)}\right)$ and van de Hulst-type near-field $\left(\sigma_k^{(N\ Field)}\right)$ cross-sections arising when $k \to 0$ and $k \to \infty$, respectively, with the following harmonic interpolation:

$$\frac{1}{\sigma_k^{(p')}} = \frac{1}{\sigma_k^{(F\ Field)}} + \frac{1}{\sigma_k^{(N\ Field)}}, \quad (4)$$

where $\sigma_k^{(F\ Field)}$ and $\sigma_k^{(N\ Field)}$ are given in Ref. 25. These terms depend on the atomic mass A and elastic constant K of the matrix in which the scatter is embedded, with A and K different from those of the matrix by the quantities ΔA and ΔK, respectively.[18] In Eq. 4, the fourth-power dependence of the Rayleigh-type cross-section $\sigma_k^{(F\ Field)} \sim \chi^4$ holds when $k \to 0$, where $\chi = k\bar{R}$ is the average scatter size parameter. Moreover, the near-geometrical cross-section $\sigma_k^{(N\ Field)}$ tends to the constant $2G = 2\pi\bar{R}^2$, when $k \to \infty$. This constant is equal to twice the projected scatter area G according to the extinction paradox.[26,27] From the precedent, an overestimate λ_{max} of the thermal conductivity is computed. Only the acoustic-like part $\sigma_{k,m}^{(ac)}$ of $\sigma_{k,m}^{(p')}$ in Eq. 4 has to be calculated in the first half BZ to obtain $\tau_{k,m}^{(ac)} > \tau_{k,m}^{(p')}$ for any mode (k, m). As a result, in accordance with the analytical developments in Ref. 25, the proportionality factor k^4 in $\sigma_k^{(F\ Field)}$ (Eq. 4) can be substituted by $(\omega_{k,m}/v_{k,m})^4$, while $\sigma_k^{(N\ Field)}$ is not related to the Debye approximation, as derived in Ref. 18. This substitution leads to scatter cross-sections $\sigma_{k,m}^{(p')} \equiv \sigma_{k,m}^{(ac)}$ and relaxation times $\tau_{k,m}^{(p')} \equiv \tau_{k,m}^{(ac)}$ in Eq. 4 showing a full modal dependency on both k and m and avoids underestimation of λ in Eq. 1. From our calculations, expect at low frequencies for the modes that are not related to thermal transport in solids, a strong predominance of $\sigma_k^{(N\ Field)}$ over $\sigma_k^{(F\ Field)}$ is observed. We obtain $\sigma_{k,m}^{(N\ Field)} \gg \sigma_{k,m}^{(F\ Field)}$ for k-values that are already below the middle location of the first folded BZ with $k = \pi/(2d)$, where $\sigma_{k,m}^{(p')}$ is small.[18] Predominance of the near-field effect is consistent with the incoherent scattering model used in this paper.

NUMERICAL RESULTS

Increasing Filling Ratio x for a Constant QD Average Distance d

As detailed in the "Atomic-Scale 3D Phononic Crystal Model" section, an upper limit λ_{max} of the thermal conductivity λ is computed as a function of the equilibrium temperature T. Indeed, an incoherent approach is used to obtain the scattering cross-sections. This approximation also leads to an overestimate $\langle l(T)\rangle_{max}$ of the effective phonon MFP. In contrast, the predicted effective product $\langle (Cv)(T)\rangle$ of the mode heat capacities by their group velocities is not maximized. Indeed, the latter is independent of the phonon relaxation times, as given by the following relationships:

$$\lambda(T) = \frac{1}{3}\langle l(T)\rangle\langle (Cv)(T)\rangle \text{ with } \langle Cv(T)\rangle = \sum_{m=1}^{N_m}\int_0^{k_{max}} |v_{k,m}|\hbar\omega_{k,m}\frac{\partial n_{k,m}^{(0)}(T)}{\partial T}g_k\,dk. \quad (5)$$

From the formulations of $\langle Cv \rangle$ (Eq. 5) and $\lambda(T)$ (Eq. 1), $\langle l \rangle_{\max}$ is computed as

$$\langle l(T) \rangle = \frac{3\lambda(T)}{\langle (Cv)(T) \rangle}, \tag{6}$$

where $\langle l(T) \rangle$ is maximized for all T-values using the incoherent scattering approach presented in the "Shrunk Relaxation Times from Incoherent Scattering" section for the relaxation times.

The dashed-dotted, dashed, and solid black curves from the top to the bottom in Fig. 3a present three computed thermal-conductivity curves of $\lambda_{\max}$ with respect to the equilibrium temperature T. They are obtained for three different types of atomic-scale 3D phononic crystals with a constant reduced supercell parameter $N = 7$. However, they show variable odd values of the reduced QD basis M and correspond to the smallest ($M = 1$), middle ($M = 3$), and largest ($M = 5$) QD sizes, respectively. Curves of $\lambda_{\max}$ versus T for two other Si/Ge supercrystal types with the same constant $N = 7$ are displayed using dashed-dotted and dashed light (grey) curves from the top to the bottom in Fig. 3a. These nanomaterials have even M-values of $M = 2$ and $M = 4$, respectively. The (red) circles (joined by a dashed curve with the same light color) denote experimental measurements of the thermal conductivity of bulk dc Si in Ref. 28 for comparison. The light (blue) dashed horizontal line (Fig. 3a) is a reference to the extreme low limit of amorphous bulk Si with an asymptotical value around 1 W/m/K when $T \geq 300$ K according to the Einstein model in Ref. 20. From the same figure, the reader can observe the strongest λ decrease for the Si/Ge QD supercrystal with the largest QD filling ratio $x = 48.5$ Ge at.% related to the model parameter $M = 5$. The latter shows a thermal conductivity that can be lower than $\lambda_{\max} = 0.2$ W/m/K at $T = 300$ K. This value is about 5 times smaller than the extreme amorphous Si limit and 750 times smaller than the experimental thermal conductivity (150 W/m/K) of bulk dc Si at room temperature. This amorphous limit is also beaten by another Si/Ge QD supercrystal with a lower filling ratio of $x = 26.5$ Ge at.% or $M = 4$, as shown by the light (gray) dashed curve in the bottom of Fig. 3a. The latter presents $\lambda_{\max} = 0.7$ W/m/K at $T = 300$ K. In contrast, when $x = 12.5$ Ge at.% (i.e., $M = 3$) and below this value, $\lambda_{\max}$ versus T is above 1 W/m/K from low to usual operation temperatures of thermoelectric devices (superior part of Fig. 3a). In fact, incoherent scattering becomes less significant when the Ge QDs are smaller and the phonon group velocities increase as well. Figure 3a also shows in the top part that the slope of the thermal conductivity of bulk dc Si versus T is larger than those of the Si/Ge QD supercrystals when T is below 20 K. Indeed, boundary scattering becomes predominant owing to the quite large effective MFP of bulk dc Si.

Figure 3b shows the five curves of the maximized effective MFPs $\langle l \rangle_{\max}$ with respect to T (Eq. 6). This

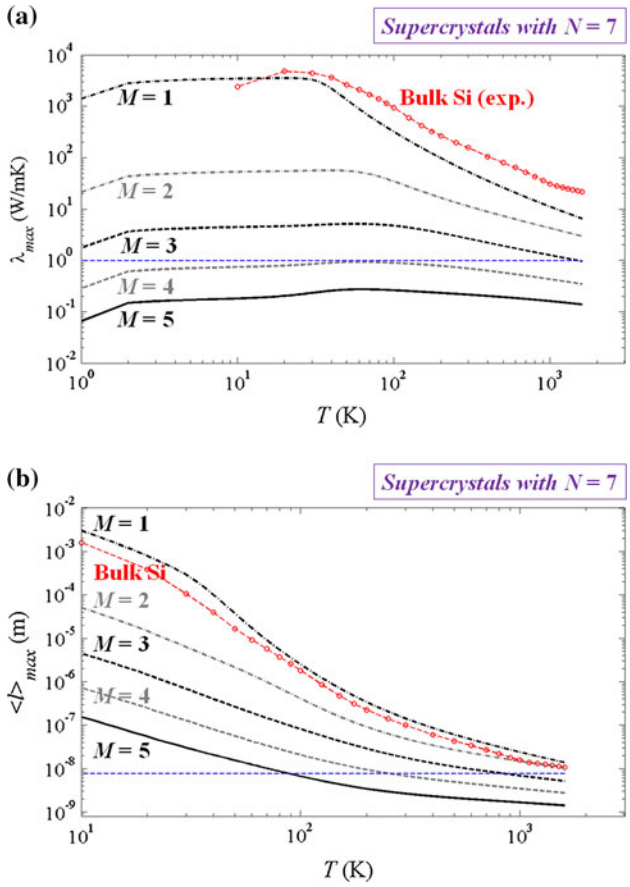

Fig. 3. (Color online) (a) Maximized thermal conductivity $\lambda_{\max}$ versus T for five atomic-scale 3D phononic crystals with $N = 7$: From the top to the bottom, the three black curves displayed by the dashed-dotted, dashed, and solid lines are for odd M-values ($M = 1$, $M = 3$, and $M = 5$, respectively). The two light (gray) curves shown by the dashed-dotted and dashed lines are for even M-values ($M = 2$ and 4, respectively). The light (blue) dashed horizontal line in (a) is a reference to the Einstein limit (of the amorphous Si thermal conductivity). Circles, joined by the light (red) dashed line, are experimental measurements of the bulk dc Si thermal conductivity versus T. (b) Maximized effective MFP curves $\langle l \rangle_{\max}$ versus T are displayed by the dashed-dotted, dashed, and solid black lines for odd M-values ($M = 1$, $M = 3$, and $M = 5$, respectively) from the top to the bottom. The two light (gray) curves shown by the dashed-dotted and dashed lines are for even M-values ($M = 2$ and $M = 4$, respectively). Circles, joined by the light (red) dashed line, give the bulk dc Si effective MFP versus T. The light (blue) dashed horizontal line in (b) is a reference to the minimal unfolded phonon wavelength of $2d = 7.6034$ nm when $N = 7$ for comparison.

figure has to be matched up with Fig. 3a. The same conventions of color and hatching as utilized in Fig. 3a are used in the latter figure to relate the five example Si/Ge QD supercrystals with $M = 1$ to 5 (and constant $N = 7$). A monotonic decrease of $\langle l \rangle_{\max}$ versus T can be seen for all examples owing to umklapp scattering (Fig. 3b). Moreover, in the bottom part, significant incoherent scattering is observed from the $\langle l \rangle_{\max}$ dependence of the two QD supercrystals with the largest QD filling ratios $x = 26.5$ Ge at.% ($M = 4$) and $x = 48.5$ Ge at.% ($M = 5$), which were also highlighted for the thermal conductivity (Fig. 3a). For these two

supercrystals, $\langle l \rangle_{max}$ becomes lower than the shortest unfolded phonon wavelength of $2d$ = 7.6034 nm, referenced by the light (blue) horizontal dashed line, when $T \geq 300$ K and $T \geq 100$ K, respectively (Fig. 3b). These results are in agreement with the utilized incoherent scattering model (see the "Shrunk Relaxation Times from Incoherent Scattering" section).

Increasing QD Average Distance d for a Constant Filling Ratio x

In this final discussion, an extreme reduction of the thermal conductivity λ to a value that can be lower than 0.04 W/m/K is predicted at T = 300 K. This extremely small value, which is lower than twice the thermal conductivity of air, can be obtained for different pairs of the size parameters d and x in the Si/Ge QD supercrystal (related to N and M/N in reduced values, respectively). This prediction might have a significant impact on thermoelectrics. Indeed, ZT depends on $1/\lambda$ (see the "Introduction"). The following results can be extended over a wide temperature range using the T-dependent model described above.

As shown in Fig. 4, at room temperature (T = 300 K), λ shows a power-law decrease with increasing QD average distance given by $d = Na$ (see the "Confinement from Flat Dispersion Curves" section) in the 3D Si/Ge supercrystal. Two example curves in black and light (grey) colors are displayed for corresponding chosen x-values of 12.5 Ge at.% and 48.5 Ge at.% (functions of the ratio M/N).

The two curves of λ versus d, plotted with respect to a double-logarithm scale, are obtained by linear interpolations of computed λ-values using the presented model. They are denoted by circles and squares for x = 12.5 Ge at.% and x = 48.5 Ge at.%, respectively (Fig. 4). For the largest x = 48.5 Ge at.% (squares), λ already reaches the value of 0.04 W/m/K for an average QD distance of $d = Na$ = 7.6 nm (i.e., N = 14 in number of interatomic distances). This d-value corresponds to an average Ge QD basis $w = Ma$ = 5.4 nm (i.e., M = 10). However, for the lowest x = 12.5 Ge at.% (circles), d has to increase to 19.6 nm (i.e., N = 36) in order to decrease λ down to the same 0.04 W/m/K value. The latter (d = 19.6 nm, x = 48.5 Ge at.%) doublet is related to the average Ge QD basis w = 9.2 nm (i.e., M = 17). This result gives a good trend for forthcoming fabrication of a Si/Ge QD supercrystal using the same order of magnitude for the parameters (d, x) as well as current technologies.

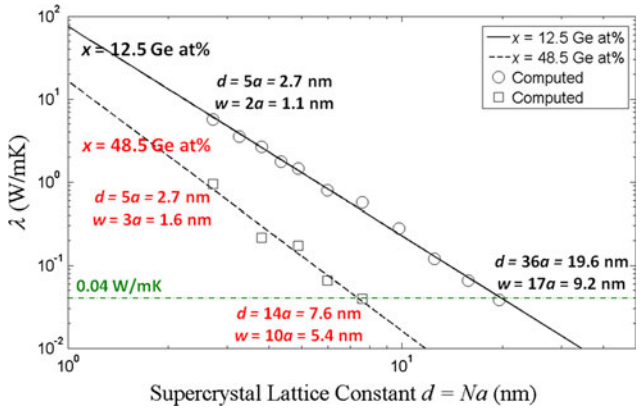

Fig. 4. (Color online) (a) Thermal conductivity λ versus average distance $d = Na$ between the quantum dots (QDs) for two sets of supercrystals with nonvariable Ge filling ratios x (related to the M/N ratio) at T = 300 K: The power-law curves of λ versus d are obtained for x = 12.5 Ge at.% (black solid line) and x = 48.5 Ge at.% (black dashed line). They are the respective interpolations of the computed data denoted by circles and squares for Si/Ge QD supercrystals with the corresponding x = 12.5 Ge at.% and x = 48.5 Ge at.%.

The computed thermal conductivity of 0.04 W/m/K shows agreement with experimental results obtained in Ref. 6 for disordered 2D WSe_2 layered crystals. Owing to the two scales of texture in the three spatial dimensions of the Si/Ge QD supercrystal (with folded wavelengths smaller than the double distance $2d$), the phonons are trapped between the Ge QDs. This phenomenon is a consequence of significant nonfocusing and localization effects, as obtained with the proposed model. Similar effects were observed experimentally in the W/WSe_2 system in Ref. 6. When disordering in the W/WSe_2 superlattice to form 2D layered crystal pieces is significantly increased (due to large ion doses), the material becomes almost amorphous. Therefore, new random thermal paths are generated and the thermal conductivity increases with respect to the supercrystal case.[6] This theoretical research also shows (from the examples of the Si/Ge QD supercrystal) that an extreme reduction of the thermal conductivity could be obtained independently of the chemical composition of the semiconductor pair used to design a supercrystal with two scales of texture.

CONCLUSIONS

An extreme reduction of the thermal conductivity λ of 3D silicon-based supercrystals with SA Ge QDs is shown based on an atomic-scale 3D phononic crystal model. Significant size and temperature effects on the λ-values are discussed. One of the most remarkable results concerns the extreme lowering of the thermal conductivity, which can be smaller than only 0.04 W/m/K at room temperature. Such an ultralow thermal conductivity is computed for size parameters of the 3D Si/Ge supercrystal in the range of current fabrication technologies, which might present significant interest for the design of very efficient thermoelectric devices. This theoretical study can be extended to a wide temperature range and shows agreement with experimental results obtained for disordered 2D W/WSe_2 layered crystals.[6] Finally, the extreme thermal-conductivity

reduction is expected to be a general property of 3D QD supercrystals, independently of the semiconductor pair used for their design.

ACKNOWLEDGEMENTS

In the framework of this research work, Dr. Gillet received the Outstanding Scientific Paper Award of the 28th International Conference on Thermoelectrics (ICT 2009) from the International Thermoelectric Society (ITS).

REFERENCES

1. W. Kim, J. Zide, A. Gossard, D. Klenov, S. Stemmer, A. Shakouri, and A. Majumdar, *Phys. Rev. Lett.* 96, 045901 (2006).
2. T.M. Tritt, H. Bottner, and L. Chen, *MRS Bull.* 33, 366 (2008).
3. A.I. Hochbaum, R. Chen, R.D. Delgado, W. Liang, E.C. Garnett, M. Najarian, A. Majumdar, and P. Yang, *Nature (London)* 451, 163 (2008).
4. A.I. Boukai, Y. Bunimovich, J. Tahir-Kheli, J.-K. Yu, W.A. Goddard III, and J.R. Heath, *Nature (London)* 451, 168 (2008).
5. S. Volz and G. Chen, *Appl. Phys. Lett.* 75, 2056 (1999).
6. C. Chiritescu, D.G. Cahill, N. Nguyen, D. Johnson, A. Bodapati, P. Keblinski, and P. Zschack, *Science* 315, 351 (2007).
7. K.F. Hsu, S. Loo, F. Guo, W. Chen, J.S. Dyck, C. Uher, T. Hogan, E.K. Polychroniadis, and M.G. Kanatzidis, *Science* 303, 818 (2004).
8. T.C. Harman, P.J. Taylor, M.P. Walsh, and B.E. LaForge, *Science* 297, 2229 (2002).
9. V.K. Zaitsev, *CRC Handbook of Thermoelectrics*, ed. D.M. Rowe (CRC Press, 1995), Chap. 25.
10. R. Venkatasubramanian, E. Siivola, T. Colpitts, and B. O'Quinn, *Nature (London)* 413, 597 (2001).
11. R. Venkatasubramanian, ed., *Nanoscale Heat Transport—From Fundamentals to Devices* (Mater. Res. Soc. Symp. Proc., Vol. 1172E, Warrendale, PA, 2009).
12. P.W.K. Rothemund, *Nature (London)* 440, 297 (2006).
13. V. Maurice, G. Despert, S. Zanna, M.-P. Bacos, and P. Marcus, *Nat. Mater.* 3, 687 (2004).
14. A. Condon, *Nat. Rev. Genet.* 7, 565 (2006).
15. C.R. Martin and P. Kohli, *Nat. Rev. Drug Discov.* 2, 29 (2002).
16. A.I. Yakimov, A.V. Dvurechenskii, and A.I. Nikiforov, *J. Nanoelectron. Optoelectron.* 1, 119 (2006).
17. S. Kiravittaya, H. Heidemeyer, and O.G. Schmidt, *Appl. Phys. Lett.* 86, 263113 (2005).
18. J.-N. Gillet, Y. Chalopin, and S. Volz, *ASME J. Heat Transfer* 131, 043206 (2009).
19. J.-N. Gillet, Outstanding Scientific Paper Award, *Proc. 28th International Conference on Thermoelectrics (ITC 2009)*, ed. H. Bottner (Freiburg, Germany, 26–30 July 2009).
20. D.G. Cahill, S.K. Watson, and R.O. Pohl, *Phys. Rev. B* 46, 6131 (1992).
21. T.T.M. Vo, A.J. Williamson, V. Lordi, and G. Galli, *Nano Lett.* 8, 1111 (2008).
22. M.T. Dove, *Introduction to Lattice Dynamics*, Cambridge Topics in Mineral Physics and Chemistry, No. 4 (Cambridge, UK: Cambridge Univ. Press, 1993).
23. Z. Jian, Z. Kaiming, and X. Xide, *Phys. Rev. B* 41, 12915 (1990).
24. Y. Chalopin, J.-N. Gillet, and S. Volz, *Phys. Rev. B* 77, 233309 (2008).
25. W. Kim and A. Majumdar, *J. Appl. Phys.* 99, 084306 (2006).
26. C.F. Bohren and D.R. Huffman, *Absorption and Scattering of Light by Small Particles* (New York: Wiley, 1998).
27. H.C. van de Hulst, *Light Scattering by Small Particles* (New York: Dover, 1981).
28. C.J. Glassbrenner and G.A. Slack, *Phys. Rev.* 134, A1058 (1964).
29. G.A. Slack and S. Galginaitis, *Phys. Rev.* 133, A253 (1964).